Tunable electronic bands in twisted bilayer $NbSe_2$

Conan Birkett

Department of Physics, University of Bath, Bath BA2 7AY, United Kingdom

August 4, 2022

Abstract

Following observation of unconventional superconductive effects in twisted bilayer graphene, the novel field of 'twistronics' has seen a rapid progression in theory and experiment. When a van der Vaals heterostructure formed from a bilayer of 2D lattices is twisted at a so-called 'magic-angle' perturbation effects and interlayer tunneling lead to the formation of a flat electronic band at fermi level in some materials. These exotic electronic properties have the potential to be exploited as high temperature superconductors or in novel electronic devices. Using a multiorbital tight binding model (TBM) we model a bilayer of transition metal dichalcogenide 2H-$NbSe_2$ with interlayer tunneling at various twist angles. We observe ***** in the electronic band structure at *** points. Our results show potential for further modelling of the $NbSe_2$.

Introduction

In 2018 Cao Y. et al[1] realised unconventional superconductivity in bilayer graphene twisted to the 'magic-angle' of 1.1°. This catapulted interest and research into graphene and two dimensional (2D) materials to new heights. The potential of graphene in realising new electronic properties and phases of matter has been extensively explored both theoretically and experimentally. In recent years, focus has been directed at electrical properties of other 2D materials like transition metal dichalcogenides (TMDCs), and how combining multiple layers of 2D materials into van der Waals heterostructures can drastically effect their electronic properties. In particular a novel field, dubbed 'twistronics' has grown from research into how relative inter-layer twist in a van der Waals heterostructure influences the electronic properties of an electronic device. We examine such a heterostructure constructed from a bilayer of 2-hexagonal niobium diselenide (2H $NbSe_2$); its monolayer is known to have different electronic properties from a bulk substrate - in particular a strong Ising-type spin orbit coupling that locks electron spins into out-of-plane directions. We show that at some twist angles there is a significant projection of low energy electronic bands onto unperterbed states (those with no interlayer coupling) at saddle points between the Γ and K critical points. This also produces nearly flat bands at relatively large twist angles near the Fermi level. The high density of states assosciated with flat electronic bands at fermi level is well studied in the context of novel electronic properties in other materials [] - in particular magic-angle superconductivity in graphene []. Experimentally, it is possible to shift the Fermi level in a 2D system by a few hundred MeV by 'sandwiching' it within a capacitor []. Additionally, the large twist angle (compared to magic-angle graphene) at which these effects are observed could be more convenient for experimental realisation. Our results thus suggest tunable novel electronic properties in bilayer $NbSe_2$ that are within experimental reach. However, further work is required in modelling the bilayer as our results use many non-trivial approximations. Significant improvements to the modelling of inter-layer tunneling can be made, and may have a drastic effect on the results presented. Regardless, our results are promising and justify further research into twisted bilayer $NbSe_2$.

perturbation theory for two levels cross and seperate

two states cross - interact and split - the stronger the coupling the further the split

compare same twist angle with higher coupling - can see bands seperate apart the levels are not degenerate but close - coupling makes them push apart by perturbation

compare rotation at same strength

for above can do 4 graphs of each maybe

at saddle point, interesting things do not happen only at small twist angles

could plot surfaces - where do they cross? at 15 degrees is it closer to saddle points?

if you can induce flatness (eg at 15 degrees some areas look flatter) in the electronic bands - leads to a high density of states (singularity - formally mathematically it tends to infinity) lots of electrons at this energy

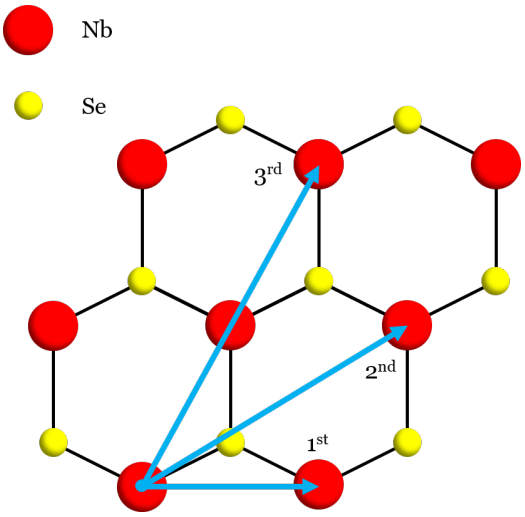

(a) Top view of $NbSe_2$ with example nearest neighbours (NN) up to third NN sites.

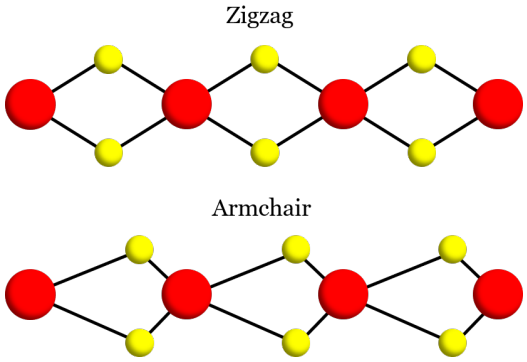

(b) Side view of $NbSe_2$ from the 'zigzag' and 'armchair' edges, Se atoms are directly above and below each other in out-of-plane axis.

Figure 1: Monolayer $NbSe_2$

flatness due to twist angles -> high density of states -> possible interesting effects

tunable! can change the properties of the material other than its metallic state normally - novel behaviour in the material is a good conclusion

figure font shouldnt be smaller than normal text - should probably be larger

Method

Our work draws on several published methods on NbSe2 and twistronics. In particular we draw upon the multiorbital tight binding model of monolayer NbSe2 from Habara and Wakabayashi[2]. To model the bilayer with twist, we employ the method used in the original magic-angle paper by Bistritzer and MacDonald [3].

Monolayer NbSe2

$NbSe_2$ is a two dimensional (2D) transition metal dichalcogenide (TMDC). Specifically it is a group-V TMDC with formula MX_2 for $M =$ Nb, Ta and $X =$ S, Se. It has metallic properties with superconductivity at temperatures below 7.2 K []. It also exhibits a strong spin orbit coupling (SOC) field which results in Ising-type spin orbit coupling, i.e. strong effective Zeeman field, which holds electron spins in out-of-plane directions. We employ a multiorbital tight binding model (TBM) of NbSe2 as described by Habara and Wakabayashi [2]. We take a basis of d_{z^2}, $d_{x^2-y^2}$ and d_{xy} orbitals of the Nb atoms with spin orbit coupling. These states are dominant in the electronic band near fermi level. This basis is suitable for modelling the behaviour of low energy electronic states in a $NbSe_2$ monolayer [].

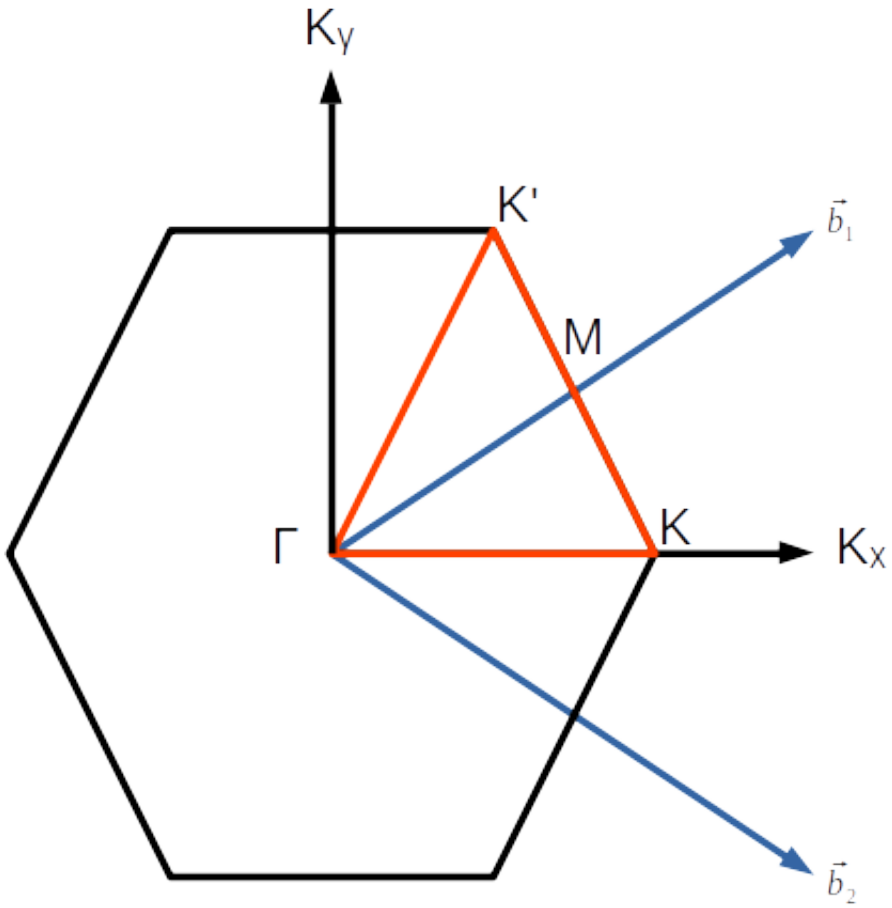

Figure 2: First Brilloin zone in a hexagonal lattice. shown are: reciprocal lattice vectors b_1, b_2, standard critical points Γ, K, K', M and wavevector axes k_x, k_y. Electronic bands are found for k sampled from the equilateral triangle $\Gamma \to K \to M \to K' \to \Gamma$ or $\Gamma \to \Gamma$ shown in red.

The TBM considers the interactions of these electronic states up to the third nearest neighbour sites.

The eigenvalue equation of the TBM is

$$\hat{H}(k)\left|u_{nk}\right\rangle = E_{nk}\left|u_{nk}\right\rangle, \tag{1}$$

where $k = (k_x, k_y)$ is the wave-number vector, E_{nk} is the eigenvalue and $n = 1, 2, \cdots, 6$ is the band index.

we define the eigenvector as

$$\begin{aligned}\left|u_{nk}\right\rangle = (&c_{nk,d_{z^2},\uparrow}, c_{nk,d_{xy},\uparrow}, c_{nk,d_{x^2-y^2},\uparrow},\\ &c_{nk,d_{z^2},\downarrow}, c_{nk,d_{xy},\downarrow}, c_{nk,d_{x^2-y^2},\downarrow})^T\end{aligned} \tag{2}$$

where $(\cdots)^T$ indicates the transpose of the vector and $c_{nk\tau s}$ is the amplitude at atomic orbital τ with spin s for the nth energy band at k.

The monolayer Hamiltonian $\hat{H}(k)$ with spin orbit coupling is then

$$\hat{H}(k) = \hat{\sigma}_0 \otimes \hat{H}_{\text{TNN}}(k) + \hat{\sigma}_z \otimes \frac{1}{2}\lambda_{\text{SOC}}\hat{L}_z \tag{3}$$

with the TBM nearest neighbour Hamiltonian

$$\hat{H}_{\text{TNN}}(k) = \begin{pmatrix} V_0 & V_1 & V_2 \\ V_1^* & V_{11} & V_{12} \\ V_2^* & V_{12}^* & V_{22} \end{pmatrix} \tag{4}$$

and spin orbit coupling term

$$\hat{L}_z = \begin{pmatrix} 0 & 0 & 0 \\ 0 & 0 & -2i \\ 0 & 2i & 0 \end{pmatrix} \tag{5}$$

$\hat{\sigma}_0$ and $\hat{\sigma}_z$ are Pauli matrices and $\lambda_{\text{SOC}} = 0.0784$ eV is the Ising-type spin orbit coupling parameter. The potentials $V_0 \cdots V_{22}$ in the TNN Hamiltonian are functions of k determined from the nearest neighbour hopping vectors with fitting parameters.

The resulting monolayer Hamiltonian $\hat{H}(k)$ is a 6x6 block diagonal Hermitian matrix as a function of wavevector k. The eigenvalues of this Hamiltonian correspond to the energy of the 6 eigenstates / electronic bands for a given point in reciprocal space k. When determining the electronic bands, we take k from slices in the first Brillouin zone along the standard critical points: Γ, K, K', M. By Bloch's theorem we can describe the electronic properties of the whole monolayer by considering the region bounded by these points due to the periodicity of potentials in the lattice and reflectional symmetry. Specifically, k bounded by the equilateral triangle $\Gamma \to K \to M \to K' \to \Gamma$, hereafter refered to as $\Gamma \to \Gamma$.

Modelling a twist

Before constructing a twisted bilayer, we first consider a monolayer twisted by some angle $theta$. A rotation in primitive lattice vectors $a_1, a_2 \to a_1', a_2'$ corresponds to the same rotation in reciprocal lattice vectors $b_1, b_2 \to b_1', b_2'$. We can treat this rotation as a rotation of the coordinate system in k space: $(k_x, k_y) \to (k_x', k_y')$. Then, for some vector $k' \in (k_x', k_y')$ we can find the same vector k' in our original wavevector basis (k_x, k_y) by rotating it by $-\theta$.

If we consider the equilateral triangle in reciprocal space $\Gamma \to K1 \to M1 \to K1' \to \Gamma$ taken on an unrotated basis, we can construct a rotated triangle $\Gamma \to K2 \to M2 \to K2' \to \Gamma$. For the the evaluation of electronic bands in a twisted bilayer we sample k from the path $\Gamma \to K1 \to M1 \to K1' \to \Gamma \to K2 \to M2 \to K2' \to \Gamma$, or in shorthand $\Gamma \to \Gamma \to \Gamma$

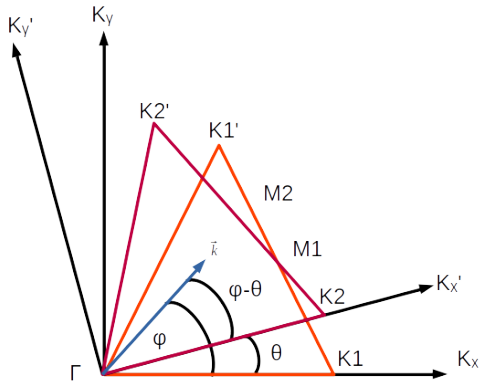

(a) Equilateral triangle from first Brillouin zone shown in unrotated and relatively rotated (by angle θ) reciprocal coordinate systems. An arbitrary vector k in the rotated basis (k'_x, k'_y) must first be rotated by $-\theta$ before it can be projected onto the unrotated basis (k_x, k_y)

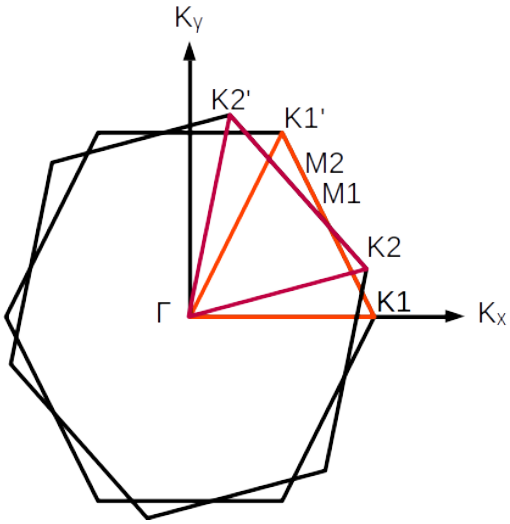

(b) Brillouin zones of both layers at relative angle θ overlayed. Evaluation of the electronic bands is taken on the set $\Gamma \to K1 \to M1 \to K1' \to \Gamma \to K2 \to M2 \to K2' \to \Gamma$ or $\Gamma \to \Gamma \to \Gamma$.

Figure 3

Twisted bilayer

$NbSe_2$ monolayers are held together by a weak van der Waals interaction. This allows for the stacking of multiple layers - specifically a bilayer. Because of the relatively weak bonding between layers it is possible to orient these layers at twist angles relative to each other. Through this rotation and by inter-layer tunneling, we aim to explore novel electronic properties in twisted bilayers.

To describe the electronic states in a twisted bilayer we can initially start with a simple model with no interaction between states in different layers. We construct the Hamiltonian of the whole system by taking a block diagonal Hamiltonian matrix $\hat{H}k$ from two monolayer matrices $\hat{H}_1 k$ and $\hat{H}_2 k'$

$$\hat{H}(\boldsymbol{k}) = \begin{pmatrix} \hat{H}_1(\boldsymbol{k}) & 0 \\ 0 & \hat{H}_2(\boldsymbol{k'}) \end{pmatrix} \tag{6}$$

where $\hat{H}_2(k')$ is the Hamiltonian of the second monolayer, which is rotated by angle θ relative to the first. To find $\hat{H}(k)$ we must rotate k to k' (as described previously) in $\hat{H}_2(k')$.

Continuing, we will denote rotated vectors as v', where the rotation is relative to a vector on the 'unrotated layer', v. We will also denote these layers by index, layer 1 is unrotated, layer 2 is rotated relative to layer 1.

Interlayer tunneling

To model inter-layer electron tunneling, we follow the method of Bistritzer and MacDonald [3] for graphene, which is outlined for a more general case by Koshino [4].

For reciprocal lattice vectors b_i, b_i' where b_i' is the equivalent reciprocal lattice vector of the rotated layer, we can show that

$$k + G = k' + G', \tag{7}$$

where $G = m_1 b_1 + m_2 b_2$ and $G' = m_1 b_1' + m_2 b_2'$ are reciprocal lattice vectors of the unrotated and rotated layers respectively.

This is because a Bloch state on layer 1 $\phi_k^{(1)}$ is a summation of $e^{i(k+b)}$ over reciprocal vectors. Similarily, on layer two $\phi_{k'}^{(2)}$ is a sum over $e^{i(k'+b')}$. The system Hamiltonian is described by Fourier components of G, G'. So the matrix element $\langle \phi_{k'}^{(2)} | \hat{H} | \phi_k^{(1)}$ is only non-zero if **??** holds. The derivation of **??** is as follows:

First we assume that equivalent unit cells in both layers X and X' have multiple atomic orbitals with real space lattice positions

$$\begin{aligned} R_X &= n_1 a_1 + n_2 a_2 + \tau_X, \\ R_{X'} &= n_1 a_1' + n_2 a_2' + \tau_{X'}, \end{aligned} \tag{8}$$

for $n_1, n_2 \in \mathrm{N}$ and primitive lattice vectors a_1, a_2 and a_1', a_2' in either layer respectively. τ_X are the sublattice positions of the atomic states in unit cell X

We define $|R_x\rangle \equiv \phi(r - R_X)$ as the atomic state of sublattice X at localised real position R_X

The interlayer Hamiltonian elements are then

$$U = -\sum_{X,X'} T_{X'X}(R_{x'} - R_x) |R_{x'}\rangle\langle R_x|, \tag{9}$$

where the inter-layer transfer potential $-T_{X'X}(R_{x'} - R_x)$ is a function of the real space positions of the atomic orbitals, the specifics of this function we shall discuss later.

We define the Bloch basis in each layer as the summation over unit cells (and thus primitive lattice vectors)

$$|k, j, l\rangle = \frac{1}{\sqrt{N_l}} \sum_{R_X} e^{ik\cdot(R+\tau_i)} \phi_j(r - R - \tau_j, z - z_l) \tag{10}$$

for wavevector k, sublattice j and layer index l where N_l is the number of unit cells in layer l. $\phi_j(r - R - \tau_j, z - z_l)$ is the wavefunction in 2d real space in the plane and out of plane.

Our inter-layer hopping Hamiltonian elements are then given by

$$\langle k', j', l'|U|k, j, l\rangle =$$

$$\frac{1}{\sqrt{N_l N_{l'}}} \sum_{R,R'} e^{ik\cdot(R+\tau_j)} e^{-ik'\cdot(R'+\tau_{j'})} \times$$
$$\langle \phi_{j'}(r - R' - \tau_{j'}, z - z_{l'})|U|\phi_j(r - R - \tau_j, z - z_l)$$

$$= \frac{1}{\sqrt{N_l N_{l'}}} \sum_{R,R'} e^{ik\cdot(R+\tau_j)} e^{-ik'\cdot(R'+\tau_{j'})} \times$$
$$t(R' - R + \tau_{j'} - \tau_j, z'_l - z_l), \quad (11)$$

where we invoke a two centre approximation, the hopping between sites is a function of their distance only. We also assume that the the hopping $t(\vec{r_{2D}}, z)$ does not depend on the direction of $\vec{r_{2D}}$ i.e. $t(\vec{r_{2D}}, z) = t(|\vec{r_{2D}}|, z)$

For a large superlattice period, the relative inter atomic positions for every combination of atomic sites are required. It is easier to reconstruct the Hamiltonian in reciprocal space.

By taking a Fourier transform (see appendix) we can show that

$$\langle k', j', l'|U|k, j, l\rangle = \sum_{G,G'} t(k' + G', z)\delta_{k-G,k'+G'}, \quad (12)$$

which yields the result in 7

As we are taking the interlayer tunneling to be a function of $k + G$, we only consider G, G' of magnitude $\leq$ the reciprocal lattice constant b. The result is that for a given k, k' we have seven pairs of permissible G, G' that obey 7 we define them as follows: G_0 is the zero vector; G_1, G_2 are equal to reciprocal lattice vectors b_1, b_2; $G_{3,\cdots,6}$ continue from reciprocal lattice vectors in a clockwise fashion in 60° intervals.

We define

$$G_i^M = G_i - G'_i \quad (13)$$

such that 7 becomes

$$k' = k + G^M \quad (14)$$

So for a given point on layer one k_0, we have a well defined set of seven permissible k' points on the second layer between which tunneling is allowed.

Previously our Hamiltonian was a 12×12 function of k. Now, with the addition of inter-layer tunneling we have an 84×84 Hamiltonian with interlayer tunneling potential on the off-diagonal blocks. We assume that the inter-layer tunneling is negligible for d_xy and $d_{x^2-y^2}$ orbitals as they exist primarily in the in-plane axis, so when constructing the Hamiltonian we only allow tunneling between d_{z^2} orbitals.

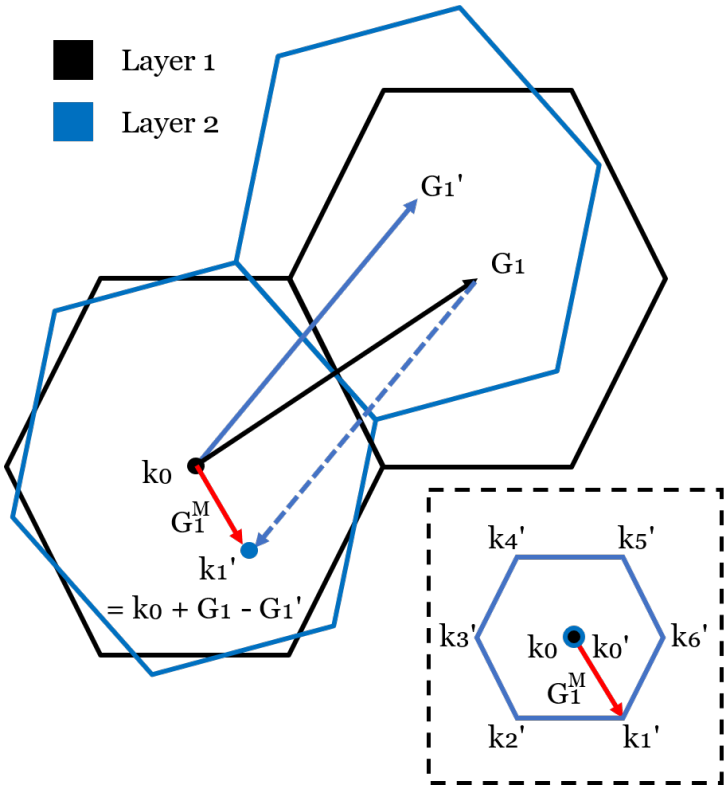

Figure 4

Tunneling potential

The tunneling potential $t(k+G,z)$ we model as a Gaussian in the in-plane axes and assume z is constant

$$t(k+G) = \frac{C\pi}{A_{UC}r_0^2} e^{-r_0^2(k+G)/4} \tag{15}$$

Due to time limitations, in our actual results we use a constant tunneling potential of 0.1eV

Implementation

The implementation of these methods and graphing of their results was done in Python using the NumPy library

Results and discussion

Monolayer electronic bands

Initially, we seek to reproduce the tight binding bands from Habara et al [2]. Using their matrix elements we reproduce the six electronic bands corresponding to the d_{z^2}, $d_{x^2-y^2}$ and d_{xy} orbitals of the Nb atoms with spin orbit coupling. The result in FIG 5 is a reproduction of the bands shown in FIG 1 d) of Habara [2]. Whilst not a novel result, it

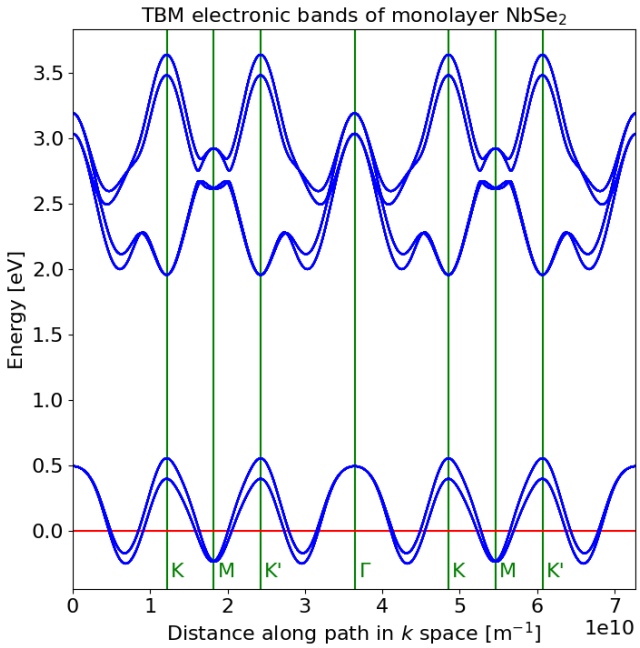

Figure 5

is a useful benchmark for checking the validity of further results. Note that Habara et al take a different path, so whilst the same bands are shown the k space axis is arranged differently. These monolayer bands predict electrical properties of monolayer $NbSe_2$, in particular that it is metallic.

Bilayer electronic bands

Following the monolayer bands, we construct a Hamiltonian of two layers, with one rotated at some twist angle θ as in eq 6. The graphs in FIG 6 show the electronic bands of both layers at 5° and 15° relative rotation on the constructed path $\Gamma \to \Gamma \to \Gamma$ seen in figure 3b. The graphs show 12 electronic bands, with 6 from each layer. Because of the construction of the path in k space, there are always 6 bands which appear exactly as in FIG 5. The remaining 6 bands are those sampled from a triangle that is rotated relative to a layer, showing discontinuity in the bands. The geometric reason for this is better seen in FIG **??**, where the above a surface plot of the lowest energy band in the same sampling region of the Brillouin zone, the band as seen in FIG 6 is shown on the triangular path it takes across the surface. Again, nothing novel can be inferred from these graphs other than that the model up to this point is functional. They simply represent two sets of electronic states corresponding to two layers of a material, with no notion of interaction, coupling, or distance between layers - only a twist relative to each other.

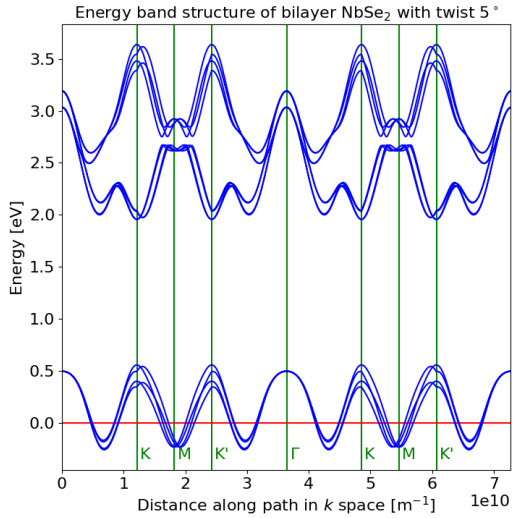

(a)

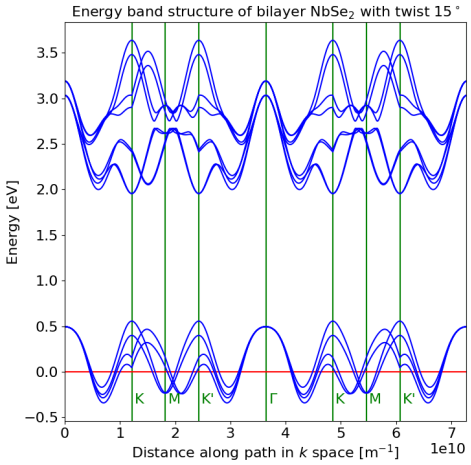

(b)

Figure 6

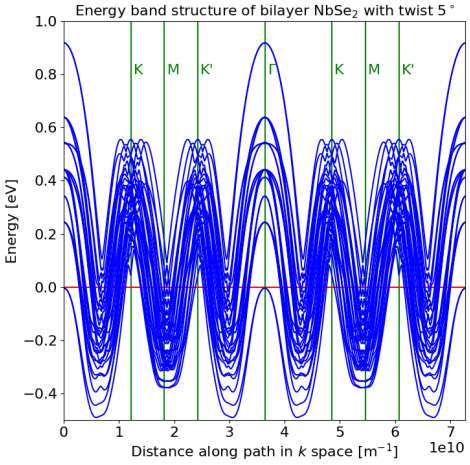

(a)

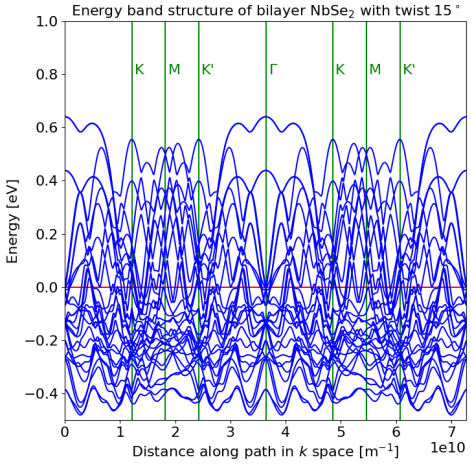

(b)

Figure 7

Inter-layer tunneling

With the model able to describe a bilayer with relative twist, we now seek to introduce some inter-layer interaction in the form of coupling by electron tunneling. From the relationship in (7) we showed that for each state at point k one one layer, there are a set of seven k' on the other layer between which tunneling is allowed. To model the tunneling between layers, we expand the Hamiltonian to describe 84 states - using a fixed tunneling coefficient of 0.1 eV for the allowed interactions. The result are 84 electronic bands, in FIG 7 we show the bands near the fermi level only. The perturbations introduced by modelling the tunneling agree

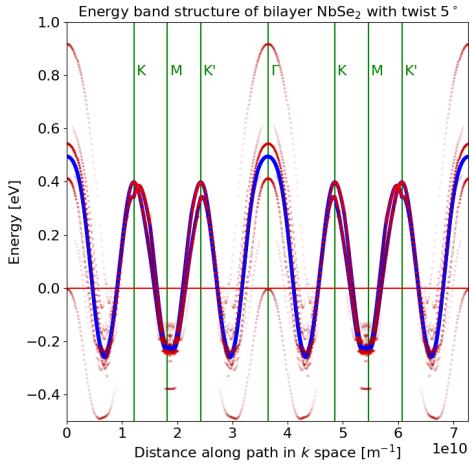

(a)

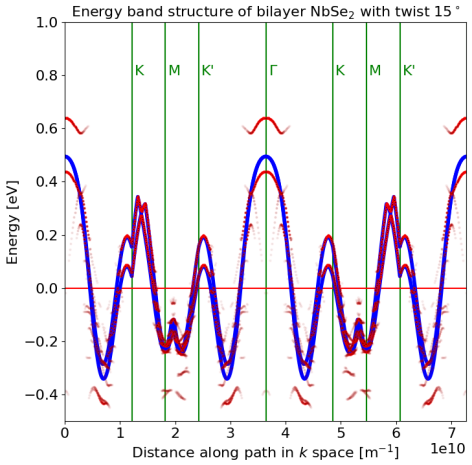

(b)

Figure 8

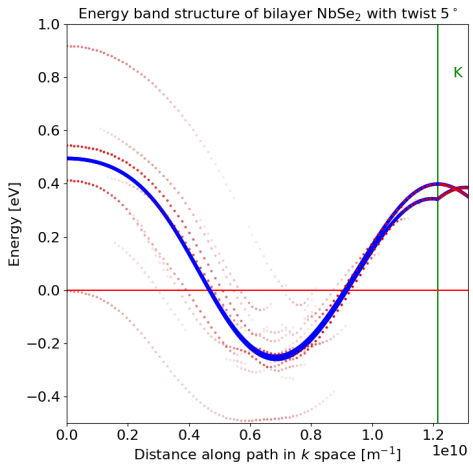

(a)

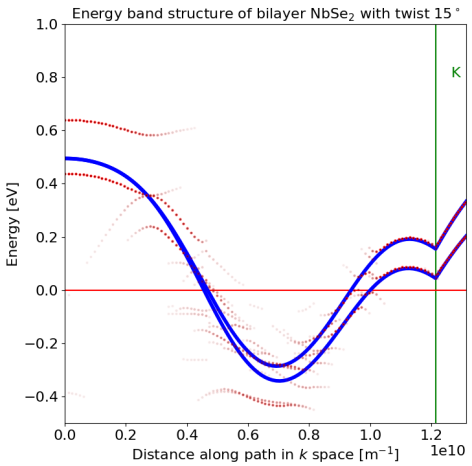

(b)

Figure 9

Discussion

Conclusions

Acknowledgements

I would like to acknowledge the contributions of my project partner Sanjana Reddy and my project supervisor Dr Marcin Mucha-Kruczynski.

Bibliography

[1] Y. Cao, V. Fatemi, S. Fang, K. Watanabe, T. Taniguchi, E. Kaxiras, and P. Jarillo-Herrero, "Unconventional superconductivity in magic-angle graphene superlattices," *Nature*, vol. 556, no. 7699, pp. 43–50, 2018.

[2] R. Habara and K. Wakabayashi, "Optically induced spin current in monolayer NbSe2," *Physical Review B*, vol. 103, no. 16, pp. 2–5, 2021.

[3] R. Bistritzer and A. H. MacDonald, "Moiré bands in twisted double-layer graphene," *Proceedings of the National Academy of Sciences of the United States of America*, vol. 108, no. 30, pp. 12233–12237, 2011.

[4] M. Koshino, "Interlayer interaction in general incommensurate atomic layers," *New Journal of Physics*, vol. 17, 2015.

Appendix

Inter-layer tunneling Hamiltonian derivation

Implementation of algorithm

The DLA data discussed in this report was generated by an implementation of the described DLA algorithm in C++. Standard C++ libraries are used for sampling of 'true' and psuedo-random numbers used in the random walk and particle generation. Utilities were written to record multiple simulations with varying parameters and to export recorded data from simulations to a csv format. Data analysis and derivation of fractal dimension was performed in Python using the numpy and pandas libraries. All computations were performed on a 64-bit desktop processor running Linux Mint 20.1 'Ulyssa'.

Note: when compiling and running the C++ code provided, the makefile in 'source' has been edited. To compile the code place the .cpp and .h files into a directory called 'source' and add in the missing/unedited files (Particle.h, Window.h, Window.cpp). Run 'make -B -C ./source/' from the directory above 'source'. The compiled binary and the data it produces are in this directory, execute the binary using './run'. The python data analysis file 'DLA.py' should also be run from this same directory

The changes made to the C++ code given by Dr A. Souslov and Dr D. Tsang are spread throughout the source code provided (i.e: CSVWrite.h, DLASystem.cpp, DLASystem.h, mainDLA.cpp, rnd.h, Makefile). Most of the changes made are used when pressing 't' in the simulation window to set parameters for data recording and P_{stick} etc. Some new functions have been added to the DLASystem class, and a new class CSVWrite is written for data recording. Some select functions are presented here but you would do best to look at the source code with comments.

```
//write recorded data to a CSV file
void DLASystem::writeDataCSV(){
  auto csv = new CSVWrite("./data.csv");

  csv->WriteVector(dataSet);
  csv->CSVClose();

  //clearDataSet();

  recording = false; //should be false anyways
}
```